Larger Numbers can Impede Adaptation in Microbial Populations despite Entailing Greater Genetic Variation

Yashraj D. Chavhan[1], Sayyad Irfan Ali[1,2], and Sutirth Dey[1,*]

[1] Indian Institute of Science Education and Research (IISER) Pune, Dr. Homi Bhabha Road, Pashan, Pune, Maharashtra, 411008, India.

[2] Indian Institute of Science, Bangalore, Karnataka, 560012, India.

*Corresponding author: Sutirth Dey, Biology Division, Indian Institute of Science-Education and Research Pune, Dr. Homi Bhabha Road, Pune, Maharashtra 411 008, India.

Conflict of interest: The authors do not have any conflict of interest.

Keywords

Predicting adaptation, effective population size, experimental evolution, extent of adaptation, population bottlenecks, adaptive size, adaptive dynamics

Abstract

Periodic bottlenecks in population sizes are common in natural (*e.g.*, host-to-host transfer of pathogens) and laboratory populations of asexual microbes (*e.g.*, experimental evolution) and play a major role in shaping the adaptive dynamics in such systems. Existing theory predicts that for any given bottleneck size (N_0) and number of generations between bottlenecks (g), populations with similar harmonic mean size ($HM=N_0g$) will have similar extent of adaptation (*EoA*). We test this widely cited claim using long-term evolution in *Escherichia coli* populations and computer simulations. We show that, contrary to the predictions of the extant theory, *HM* fails to predict and explain *EoA*. Although larger values of g allow populations to arrive at superior benefits by entailing increased number of individuals, they also lead to lower *EoA*. We also show analytically how the extant theory overestimates the effective population size relevant for adaptation. Altering the current theory using these insights, we propose and demonstrate that N_0/g (and not N_0g) successfully predicts *EoA*. Our results call for a re-evaluation of the role of population size in two decades of microbial population genetics and experimental evolution studies. These results are also helpful in predicting microbial adaptation, which has important evolutionary, epidemiological and economic implications.

Introduction

Population size is a key demographic parameter that affects several ecological and evolutionary processes including the rate of adaptation (Gerrish and Lenski, 1998; Lanfear *et al.*, 2014; Wilke, 2004; Desai *et al.*, 2007; Samani and Bell, 2010), efficiency of selection (Petit and Barbadilla, 2009), organismal complexity (LaBar and Adami, 2016), fitness decline (Katju *et al.*, 2015), repeatability of evolution (Lachapelle *et al.*, 2015; Szendro *et al.*, 2013), etc. Interestingly though, what constitutes a proper measure of population size often depends on the ecological/evolutionary question being addressed (Charlesworth, 2009). For example, for an ecologist studying population-dynamics, the total number of individuals is often the appropriate metric (Dey and Joshi, 2006). On the other hand, for a conservation biologist studying the loss of heterozygosity (Ellstrand and Elam, 1993), or an evolutionary biologist who wishes to predict how much a population would adapt over a given time relative to the ancestral state (*i.e.*, extent of adaptation or *EoA*) (Samani and Bell, 2010), the effective population size (N_e) might be a more suitable measure (Campos and Wahl, 2009; Charlesworth, 2009; Desai *et al.*, 2007; Wahl and Gerrish, 2001). Consequently, it is crucial to use the relevant measure of population size while constructing or empirically validating any evolutionary theory.

Experimental evolution using asexual microbes has been one of the key tools in validating several tenets of evolutionary theory (reviewed in (Kawecki *et al.*, 2012)). Most such studies deal with populations that face regular and periodic bottlenecks during their propagation (Kawecki *et al.*, 2012). Since the absolute population size keeps changing regularly in such experiments, the harmonic mean population size *(HM)* is often estimated as the 'effective population size' in such studies (Lenski *et al.*, 1991; Wahl and Gerrish, 2001; Campos and Wahl, 2010). Specifically, if a population grows from size N_0 to N_f via binary fissions within a growth

65 phase, and is diluted back periodically to N_0 by random sampling at the end of the growth phase,
66 then the effective population size is given by $N_e \approx N_0 * log_2(N_f/N_0) = N_0 g$, where g refers to the
67 number of generations between successive bottlenecks and $N_0 g$ is the harmonic mean size
68 (Lenski *et al.*, 1991). Other measures of the adaptively relevant population size used in
69 experimental evolution studies are conceptually similar, and are of the form $N_e = N_0 g C$, where C
70 is a constant (Desai *et al.*, 2007; Wahl and Gerrish, 2001; Campos and Wahl, 2009; Samani and
71 Bell, 2010).

72 Several experimental studies, employing a variety of asexual model organisms, have used *HM*
73 for quantifying the effective population size (Desai *et al.*, 2007; Samani and Bell, 2010; Lenski
74 *et al.*, 1991; Raynes *et al.*, 2012, 2014; De Visser and Rozen, 2005; Rozen *et al.*, 2008).
75 However, there is no direct empirical validation of the suitability of *HM* as a measure of
76 population size that can explain the *EoA*. More critically, recent findings have questioned the
77 validity of *HM* as the evolutionarily relevant measure of population size in both asexual (Raynes
78 *et al.*, 2014) and sexual (Jiménez-Mena *et al.*, 2016) organisms. Here we address this issue using
79 a combination of agent-based simulations and long-term evolutionary experiments using
80 *Escherichia coli*. We first test the suitability of *HM* as a predictor of *EoA*, and show that both
81 real bacterial as well as simulated, populations with similar values of $N_0 g$ can have markedly
82 different adaptive trajectories. Secondly, we demonstrate that although increasing the value of g
83 promotes adaptation through an increased supply of variation, it also impedes adaptation by
84 restricting the spread of beneficial mutations, brought about by reduced efficiency of selection.
85 Thus, the resultant *EoA* is an interplay between these two opposing aspects of g and contrary to
86 the extant theoretical expectations (Campos and Wahl, 2009; Heffernan and Wahl, 2002), *EoA*
87 has a negative relationship with g. Thirdly, we show that populations with similar *HM* can not

only have different fitness trajectories, but can also differ markedly in terms of how frequency-distribution of fitness amongst individuals changes during adaptation. We then show that, for a given mutation rate, N_0/g (we call this quantity the adaptive size, *AS*) is a much better predictor of *EoA* trajectories, *i.e.*, populations with similar *AS* have similar fitness trajectories and populations with higher *AS* adapt faster. Finally, we demonstrate that during adaptation, populations with similar *AS* can converge on similar trajectories of *EoA* using mutations with widely different fitness effects. Our findings challenge the current notion of how population size influences adaptation.

Materials and Methods

Experimental evolution

Selection regimens:

We propagated three distinct regimens (LL, SL, and SS) of *Escherichia coli* MG 1655 populations for more than 380 generations. 8 independently evolving replicate lines each of LL (large *HM* and large N_f, selection in flasks; culture volume: 100ml), SL (small *HM* but large N_f, selection in flasks; culture volume: 100ml), and SS (small *HM* and small N_f, selection in 24-well plates; culture volume: 1.5 ml) were derived from a single *Escherichia coli* K-12 MG1655 colony and propagated in Nutrient Broth with a fixed concentration of an antibiotic cocktail containing a mixture of three antibiotics at sub-lethal concentrations (See Supplementary Methods). The three population regimens experienced different numbers of evolutionary generations (g) between periodic bottlenecks (*i.e.*, before they were sub-cultured). SS and SL had similar *HM (i.e.*, N_0g*)* albeit obtained through different combinations of N_0 (SS>SL) and g (SL>SS) such that the N_f of SL

was approximately 73 times larger than that of SS. The N_f of SL was similar to that of LL, while the harmonic mean size of LL was > 16,500 times larger than that of SL and SS (Table S1). LL was bottlenecked 1/10 every 12 hours, SS was bottlenecked $1/10^4$ every 24 hours, and SL was bottlenecked $1/10^6$ every 36 hours. 1 ml cryostocks belonging to each of the twenty four independently evolving populations were stored periodically.

Fitness assays: To reconstruct the evolutionary trajectories of our experimental bacterial populations, we measured bacterial growth using an automated multi-well plate reader (Synergy HT, BIOTEK ® Winooski, VT, USA). Bacterial growth was measured in the same environment that the populations experienced during evolution using OD at 600 nm as a proxy for population density. Bacteria from the cryostocks belonging to each of the 24 populations were grown in 96 well plates. Each cryostock-derived population was assayed in three measurement-replicate wells in a 96 well plate. Each well contained 180 µl growth medium containing $1{:}10^4$ diluted cryostock. The plate was incubated at 37^{O}C, and shaken continuously by the plate-reader throughout the growth assay. OD readings taken every 20 minutes during this incubation resulted in sigmoidal growth curves. Fitness measurements were done using cryostocks belonging to multiple time-points in order to reconstruct evolutionary trajectories. While making trajectories, it was made sure that every 96 well-plate contained populations belonging to similar time-points (in terms of number of generations). We used the carrying capacity (K) and maximum population-wide growth rate (R) as the measure of fitness (Novak *et al.*, 2006). K of a population was defined as the maximum OD value attained over a period of twenty four hours (the highest value in the sigmoidal growth curve) while R was estimated as the maximum slope of the growth curve over a running window of four OD readings (each window spanning one hour) (Karve *et al.*, 2015; Ketola *et al.*, 2013; Vogwill *et al.*, 2016; Lachapelle *et al.*, 2015). Fitness measurements were done using cryostocks belonging to multiple time-points in order to reconstruct evolutionary

trajectories. While making trajectories, it was made sure that every 96 well-plate contained populations belonging to similar time-points (in terms of number of generations).

Statistics: Bacterial fitness was analyzed for each of the two growth parameters (*K* and *R*) using a nested-design ANOVA with population regimen-type (SS, SL or LL) as a fixed factor and replicate-line (1-8, nested in population-type) as a random factor. We corrected for the error derived from multiple tests using Holm-Šidàk correction (Abdi, 2010). Since we observed adaptive trait trajectories with curves of diminishing returns throughout our study, we used extent of adaptation (*EoA*) at any given time to compare the three regimens. Throughout this study, *EoA* refers to the amount of fitness gained with respect to the ancestor.

Simulations of microbial evolution

We simulated fission-based asexual population growth under resource limited conditions to further investigate the issue and generalize our results. In our model, an individual bacterium was characterized by three principal parameters: efficiency, threshold, and body-mass. The simulation began with a fixed amount of resources available in the environment, utilized by the bacteria for growth. A typical individual was represented by an array (coded in the C programming language) that specified three principal parameters: (1) Bodymass, (2) Efficiency, and (3) Threshold. Bacteria consumed resources in an iterative and density-dependent manner. The parameter $Bodymass_i$ of a typical individual (say individual i) represented how big the particular individual is during a given iteration. Its efficiency (K_eff_i) specified how much food it assimilated per iteration. If $population\ size/\ K\_eff_i < 1$, $10*(1 - (population\ size/\ K\_eff_i))$ units were added to $Bodymass_i$. Otherwise, $Bodymass_i$ remained unchanged. $Bodymass_i$ increased with cumulative assimilation. The moment $Bodymass_i$ becomes greater than or equal to $thres_i$ (its

threshold parameter), the individual *i* underwent binary fission and divided into two equally sized daughter individuals. Each fission event had a fixed probability of giving rise to mutations based on a mutation rate that remained constant for all individuals in the population. K_eff_i and $thres_i$ mutate independently, and were the only two parameters that could undergo mutation. The mutated value was drawn from a static normal distribution with the frequency of deleterious mutations being much higher than that of beneficial mutations, which is in line with experimental observations (Kassen and Bataillon, 2006; Eyre-Walker and Keightley, 2007). The distribution of mutational effects remained fixed throughout the simulation (Kassen and Bataillon, 2006) due to which, *EoA* was expected to eventually approach a plateau. When the population ran out of resources (once the amount of body-mass accumulated per unit time by the population went below a pre-decided threshold so that the sigmoidal curve reached a plateau), it was sampled according to the sampling ratio being studied. The above process was repeated for 400 generations, where each generation represented two-fold growth in population size (see Supplementary Methods for a detailed description of the model).

Results

HM failed to predict and explain the *EoA* trajectories of experimental populations.

HM failed to explain the *EoA* trajectories of experimental populations. In spite of having similar values of N_0g, the SL and SS regimens had markedly different adaptive *(EoA)* trajectories for *K* (Fig. 1a; See Table S3 for the *p*-values) as well as *R* (Fig. 1b; Table S4). This observation is consistent with recent empirical findings that question the validity of harmonic mean as the effective population size (Raynes *et al.*, 2014). Surprisingly, SS had a larger overall *EoA* than SL

178 despite having lower N_f. This suggests that bottleneck intensities might have a greater effect on
179 *EoA* trajectories than absolute population sizes. We grew LL as a control regimen in order to
180 address whether N_f itself could predict *EoA* trajectories. Despite having N_f similar to SL, LL
181 typically had much larger *EoA* than SL.

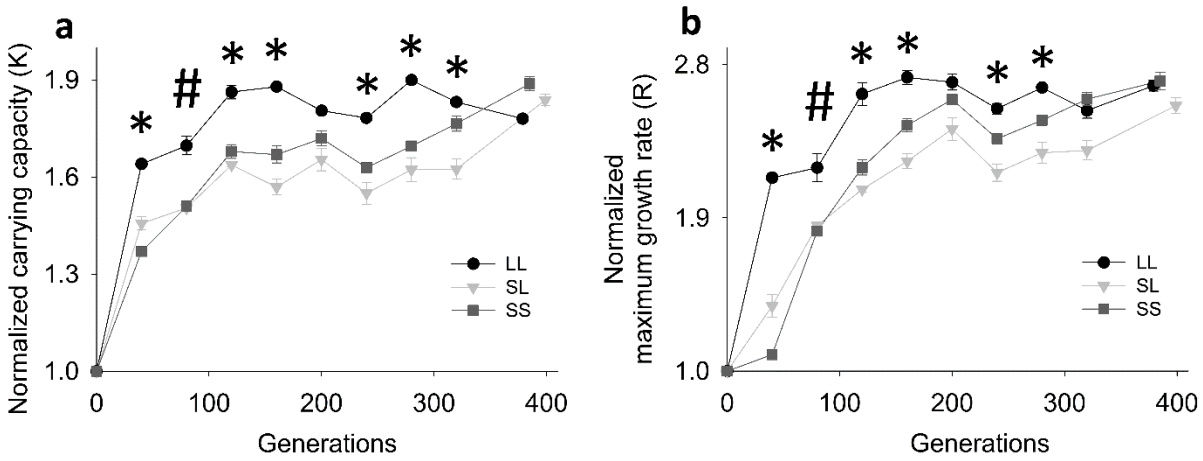

182

183 **Fig. 1. Experimental *EoA* trajectories in terms of carrying capacity and maximum growth**
184 **rate.** (**a**) *EoA* of carrying capacity *(K)*. (**b**) *EoA* of maximum growth rate *(R)***.** Data points show
185 mean ± SEM for 8 replicates. * refers to cases when all three regimens are significantly different
186 from each other (Tukey post hoc $p < 0.05$). # refers to significant difference across LL-SL and
187 LL-SS, but not SL-SS (See Tables S3 and S4). SS and SL have markedly different adaptive
188 trajectories despite having similar harmonic mean population sizes.

189

190 **Simulations also revealed that *HM* fails to explain and predict adaptive trajectories.**

191 To obtain greater and generalizable insights into the various determinants of *EoA* trajectories, we
192 used an Individual Based Model (IBM) with different values of N_0 and g, such that the product
193 (N_0g) remained similar. If N_0g were a good predictor of how much a population is expected to
194 adapt, then these three treatments were expected to show similar *EoA* (Campos and Wahl, 2009;
195 Wahl and Gerrish, 2001). This was not found to be the case for both *K* (Fig. 2a) and *R* (Fig. 2b),
196 which was consistent with our experimental observations of *EoA* trends in SL and SS (Fig. 1).

XX', SS', and SL' were also found to be remarkably different in terms of the adaptive increase in average efficiency of individuals (Fig. S4a). We also found that populations with similar harmonic mean sizes could differ remarkably in terms of the frequency distributions of the efficiency parameters amongst their constituent individuals (Fig. S5). In order to elucidate why N_0g could not explain *EoA* trajectories, we determined how *EoA* varied with N_0 and g, independently.

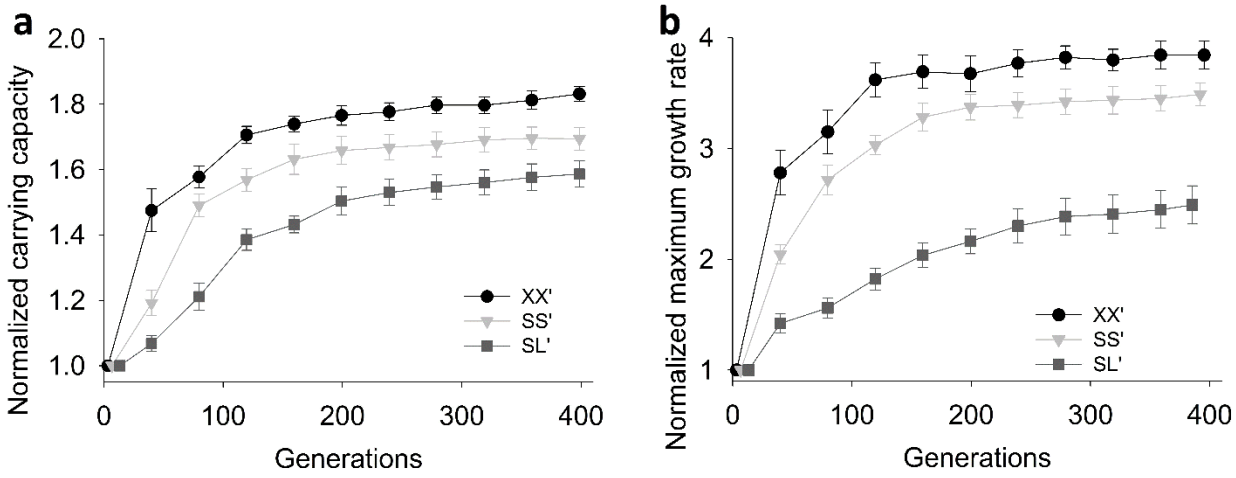

Fig. 2. Adaption in three populations with similar harmonic mean size. Data points show mean *EoA* ± SEM for 8 replicates. (**a**) Adaptation in terms of normalized carrying capacity *(K)*. (**b**) Adaptation in terms of normalized maximum growth rate *(R)*. XX', SS' and SL' had similar harmonic mean sizes and represent lenient, medium and harsh bottlenecks with $N_0 \approx 3.6*10^3$, $1.8*10^3$, $9*10^2$ and bottleneck ratio of 1/10; $1/10^2$,$1/10^4$ respectively. Populations with similar harmonic mean size can have markedly different *EoA* trajectories.

EoA varied positively with N_0 but negatively with g.

If N_0g were a good measure of the adaptation effective population size (*i.e.*, the measure of population size which has a positive relationship with *EoA* and can explain *EoA* trajectories),

then increasing either or both of N_0 and g should lead to greater *EoA*. We tested this intuitive prediction via simulations using several combinations of N_0 and g. Although *EoA* was found to increase with greater N_0 (Fig. S6a and S6b), the relationship between *EoA* and g turned out to be negative (Fig. 3; Fig. S6c and S6d). The latter result implied that large values of N_f impeded adaptation in populations even when the population size during the bottleneck (N_0) was held constant. The nature (sign) of this relationship between *EoA* and g was found to be robust to changes in mutation rate over a 100-fold range in our simulations (Fig. S7).

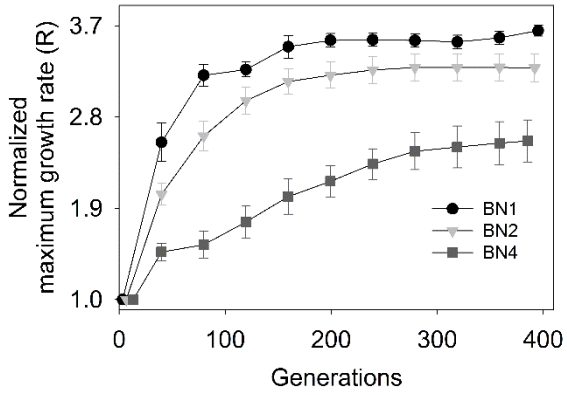

Fig. 3. *EoA* trajectories of populations with similar bottleneck size (N_0) but different bottleneck ratios. Data points show mean ± SEM; 8 replicates. All the population regimens shown here had $N_0 \approx 900$. Bottleneck ratios: BN1: 1/10; BN2: $1/10^2$; BN4:$1/10^4$. Starting $N_0 \approx 900$. Larger values of g lead to reduced *EoA* for a given number of generations.

A negative relationship between *EoA* and g is particularly surprising because, in populations with similar N_0, increase in g is expected to lead to an increase in the available variation. This is because a larger value of g automatically means an increase in N_f with a concomitant increase in the number of fissions per evolutionary generation (and hence chances of mutation). All else

being equal, this should have led to greater *EoA*. Since that was not the case, we went on to check if these slowly adapting populations (with similar N_0 but higher g values) were limited by the availability of variation, both qualitatively and quantitatively.

The availability of beneficial traits could not explain why *EoA* varied negatively with *g*.

Consider SM1 and SM4, treatment regimens which had similar starting population size (N_0) after the first bottleneck but had g values of 3.32 and 13.28 respectively (SM refers to sampling ratio, expressed in terms of log(10) (see Fig. 4 and 5). SM1 grew to a final size of $10N_0$ in one growth phase (*i.e.*, before bottleneck), while SM4 grew to 10^4N_0. In other words, SM1 faced a periodic bottleneck of 1/10 whereas SM4 was sampled $1/10^4$ periodically. Since SM4 experienced approximately 279 times more fission events than SM1 per evolutionary generation, the former was expected to undergo more mutations and consequently show more variation. Moreover, SM4 was also expected to arrive at very large-effect benefits that were so rare that the probability of SM1 stumbling upon them was vanishingly low due to its lower mutational supply. As expected, SM4 was not found to be limited by the supply of variation as it had a consistently higher within-population coefficient of variation in terms of efficiency values than SM1 (Fig. 4). SM4 also had a continual access to highly fit genotypes (Fig. 5a) that were inaccessible to SM1 throughout the simulations. On the basis of these observations, *EoA* can be expected to vary positively with g and thus SM4 was expected to be fitter than SM1 at a given point of time in general. However, counterintuitively, SM4 had a consistently lower *EoA* than SM1 (Fig. 4). Evidently, harsher periodic sampling impeded adaptation despite resulting in increased substrate for selection. We also found that although higher census size allowed SM4 to arrive at extremely rare mutations with very large benefits, these mutations failed to survive the harsh periodic bottlenecks by rising

to large enough frequencies (Fig. S8). This explains why arriving at these rare mutations with very large benefits did not make SM4 adapt more than SM1 in a sustained manner. However, this does not explain why the *EoA* in SM4 was consistently lower than that of SM1.

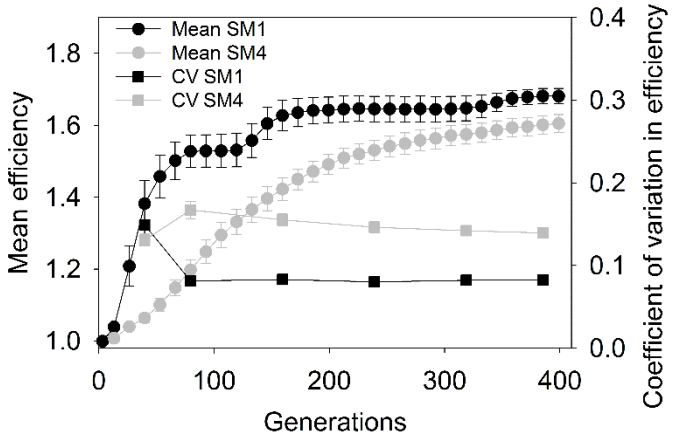

Fig. 4. Trajectories of efficiency in terms of across-population mean and within-population coefficient of variation. The within-populations coefficient of variation (CV) was computed for each replicate population across its constituent individuals using discrete frequency distributions. The error bars represent SEM (8 replicates). Both SM1 and SM4 had similar bottleneck size (N_0 ≈ 900). SM1 experienced a periodic bottleneck of 1/10 whereas SM4 experienced a periodic bottleneck of $1/10^4$. SM4 had a consistently lower *EoA* than SM1 despite having consistently more variation.

The negative relationship between *EoA* and *g* can be explained in terms of efficiency of selection.

EoA depends on an interplay between two factors: (I) generation of beneficial variation and (II) an increase in the frequency of beneficial variants as an interaction between selection and drift. The first depends upon the supply rate of beneficial mutations (Sniegowski and Gerrish, 2010), and, as shown above, the relative availability of beneficial mutations across SM1 and SM4 does not explain why SM4 was adaptively inferior to SM1. An increase in the frequency of beneficial

variants is aided by the efficiency of selection (in eliminating deleterious mutations and spreading beneficial ones), which is reflected by how quickly the modal phenotype of a population approaches its best phenotype. Since all our simulations were started with a symmetric (uniform) distribution of efficiency and threshold amongst individuals, directional selection was expected to give rise to a negatively skewed distribution of efficiency. In such negatively skewed distributions, the smaller the difference between the mode and the mean, the higher would be the efficiency of selection. Selection operated more efficiently in SM1 than in SM4 as the modal phenotypic class converged with the best available phenotypic class in most SM1 populations (as reflected by the string of zeros in SM1 (Fig. 5b)), but failed to do so in all SM4 populations. Moreover, the distance between the location of the modal class and the mean class was much smaller in SM1 as compared to SM4 (Fig. 5c).

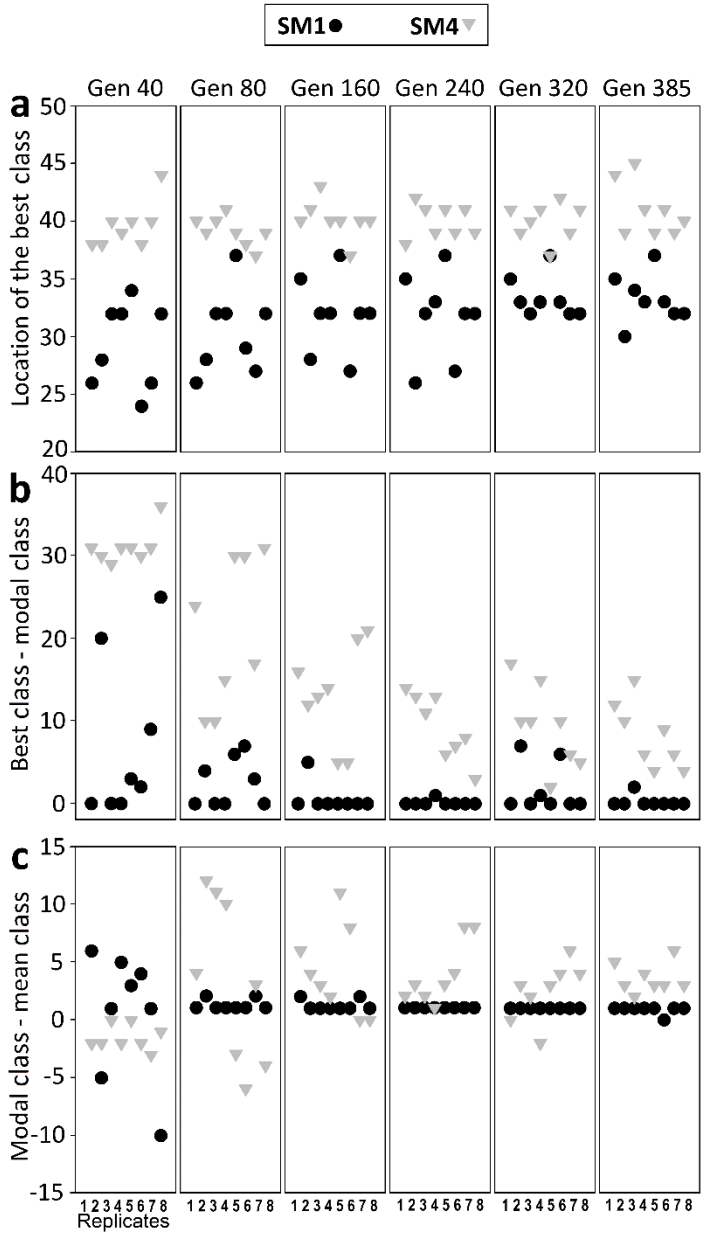

Fig. 5. Distributions of phenotypic effects across individuals during adaptation. The individuals of each simulated population (8 replicates each of SM1 and SM4) were classified into to a discrete frequency distribution of their efficiency values (50 static classes). Higher class indices correspond to higher efficiencies. (**a**) The best phenotype (in terms of efficiency) explored by SM4 was consistently fitter than the best phenotype explored by SM1. The modal phenotype quickly converged to the best available phenotype in all but one SM1 populations but failed to do so in all SM4 populations (**b**). The mean phenotype in SM1 approached the best phenotype very closely (**b and c**). However, there was a consistently larger gap between the best phenotype and the modal phenotype in SM4 (**c**) and an even larger one between its best and mean phenotype (**b and c**).

297 **N_0/g is a better predictor of *EoA* than N_0g.**

298 Since our simulations suggested that the rate of adaptation is positively related to N_0 and
299 negatively related to g, we went on to test if N_0/g is a better predictor of adaptive trajectories than
300 N_0g. N_0/g indeed turned out to be a better predictor of *EoA* trajectories not only in our
301 simulations (Fig. 2, 6, and S9), but also for our experiments. The N_0/g values of LL, SS and SL
302 populations were approximately $3.01*10^9$, $1.13*10^4$, and $5.02*10^3$, respectively, which led to a
303 predicted *EoA* trend of LL>SS>SL, which was observed for both *K* and *R* in the experiments
304 (Fig. 1). We call the quantity N_0/g the adaptive size *(AS)* and propose that *AS* should be used to
305 make predictions about *EoA* in periodically bottlenecked asexual populations. We also found that
306 populations with similar *AS* can have markedly different trait distributions at any given time
307 despite having very similar trajectories of mean fitness (Fig. S10). Evidently, similar
308 distributions of *EoA*-affecting traits amongst individuals imply similar mean *EoA* trajectories, but
309 the converse is not true. We elaborate on this result in the discussion section.

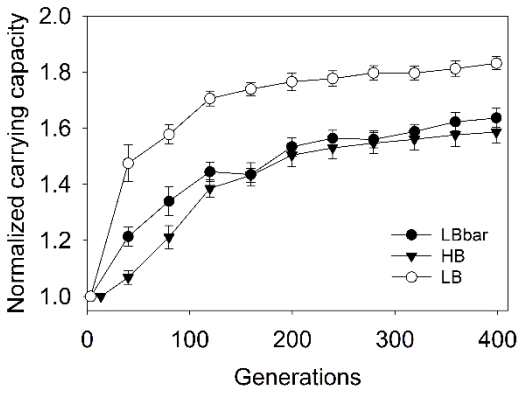

310

311 **Fig. 6. *EoA* trajectories in terms of normalized carrying capacity.** Populations with similar
312 N_0/g (LB**bar** and HB) match more closely in terms of mean adaptive trajectories than
313 populations with similar N_0g (LB and HB). LB: $N_0 \approx 3600$, bottleneck ratio: 1/10; HB: $N_0 \approx 900$,
314 bottleneck ratio: $1/10^4$; LBbar: $N_0 \approx 225$, bottleneck ratio: 1/10.

315

Discussion

Periodic bottlenecks lead to increased variation but reduced adaptation.

The growth of many natural asexual populations is punctuated by episodic bottlenecks caused by, for example, abrupt dissociation from hosts or spread of infections across hosts (reviewed in (Abel *et al.*, 2015)), etc. Moreover, periodic sampling during sub-culturing is a common feature of most asexual populations propagated during experimental evolution studies (Kawecki *et al.*, 2012; Lenski *et al.*, 1991). Therefore it is important to appreciate the complex role played by periodic bottlenecks in such populations. Most experimental evolution studies with asexual microbes are started with either genetically uniform/clonal replicate populations or a relatively small inoculum. Thus, the generation and survival of *de novo* beneficial variation is the principal basis of adaptation in such populations (Kawecki *et al.*, 2012; Barrick *et al.*, 2009). Populations that experience more binary fissions per generation are expected to generate more *de novo* beneficial variation and thus, to have a higher extent of adaptation. The number of binary fissions per generation is given by $N_0*(2^g-1)/g$ (see below), which varies positively with g (Fig. S11). Therefore, if *EoA* depends solely upon the amount of variation generated by mutations, then all else being equal, *EoA* is expected to vary positively with N_0 and g, which is consistent with the expectation that *HM* ($\approx N_0 g$) should be a good measure of the *adaptive* effective population size. However, this line of reasoning disregards the loss of variation during periodic bottlenecks, which increases in intensity with increasing g due to decrease in the fraction of the population being sampled. It has been predicted that the probability that a beneficial mutation of a given size survives a bottleneck varies negatively with the harshness of sampling (*i.e.*, increasing g) (Wahl *et al.*, 2002). However, since the overall rate of adaptation depends upon the

product of beneficial mutational supply rate and survival probability, it has also been suggested that bottlenecked populations may adapt faster than populations of constant size (Wahl *et al.*, 2002). Heffernan and Wahl have proposed that exponential growth is a more potent evolutionary force than abrupt periodic bottlenecks, and increasing *g* increases the probability of fixation of a beneficial mutation (Heffernan and Wahl, 2002). The sign of the relationship between *EoA* and *g* has not been put to empirical test yet, but, as shown above, the extant formula *(HM)* for the adaptive effective size implies a positive relationship (Campos and Wahl, 2009; Wahl and Gerrish, 2001). Our experiments (Fig. 1) and simulations (Fig. 2) did not support this prediction and *EoA* was found to have a negative relationship with *g* (Fig. 3).

In order to explain this discrepancy, we simulated populations with similar values of N_0 (*i.e.*, bottleneck size) but different degrees of harshness of the bottlenecks, namely SM1 (lenient bottleneck, g =3.32) and SM4 (harsh bottleneck, g = 13.28) (Fig. 4 and Fig. 5). The high fitness phenotypes had a higher probability of getting lost due to the harsh sampling in SM4 (1 in10^4) than in SM1 (1 in 10^1) as reflected in Fig. S8. Moreover, asexual reproduction prevents multiple alternative beneficial mutations from coming together in any given individual. Therefore, alternative beneficial mutations compete with each other for fixation. This competition, also known as clonal interference (CI), impedes the speed of increase in average population-wide fitness (Gerrish and Lenski, 1998; Wilke, 2004; Park and Krug, 2007; Sniegowski and Gerrish, 2010). This is because increasing the availability of beneficial mutations beyond a particular level does not result in a concomitant increase in adaptation rate, thus leading to a relationship of diminishing returns between adaptation-rate and beneficial mutational supply (Gerrish and Lenski, 1998). Since the intensity of CI varies positively with the number of such competing mutations (Gerrish and Lenski, 1998), the effects of CI would be much more pronounced in SM4

362 populations which have ~279-times greater number of mutations per generation compared to the
363 SM1 populations.

364

365 **N_0/g determines the amount of variation that ends up surviving the bottleneck.**

366 If binary fission is the basis of exponential growth from N_0 to N_f (one growth phase), the number
367 of fissions is given by N_f - N_0. The number of rounds of fissions that take place during this
368 growth phase is $log_2(N_f/N_0)$, which is equal to g. Therefore, the number of new mutations that
369 occur during this growth phase (from N_0 to N_f) is given by $\mu*N_0*(2^g - 1)$ where μ is the mutation
370 rate. At the end of the growth phase, the population is bottlenecked by random sampling of N_0
371 individuals. Ignoring the arrival times and fitness differences across mutations and plugging in
372 $N_f/N_0=2^g$, the number of new mutations that would putatively end up surviving this sampling
373 from N_f individuals to N_0 individuals would then be given by $(N_0/N_f)*\mu*N_0*(2^g - 1) = (2^{-g})*$
374 $\mu*N_0*(2^g - 1)$. If $2^g >> 1$ (*i.e.*, if g is large), then $2^g - 1 \approx 2^g$ and $(N_0/N_f)*\mu*N_0*(2^g - 1) \approx \mu*N_0$.
375 Populations that face different bottleneck ratios undergo different number of bottlenecks (and
376 growth phases) in a given number of generations. For example, a population that faces a periodic
377 bottleneck of $1/10^4$ undergoes 30 growth phases in 400 generations whereas a population that
378 faces a periodic bottleneck of 1/10 undergoes 120 growth phases in the same number of
379 generations. Therefore, in order to compare different populations, at a given point of time, in
380 terms of the amount of variation that survives sampling, we need to calibrate this quantity with g,
381 the number of generations per growth phase. Since the growth phase from N_0 to N_f spans g
382 evolutionary generations, the number of new mutations created per generation that would end up
383 surviving the bottleneck would be given by $\mu*N_0/g$. We acknowledge that this is a simplification

and in reality, both arrival times and mutational competition are significant factors that shape evolutionary trajectories (Sniegowski and Gerrish, 2010) (see below for further discussion).

Populations with remarkably different beneficial mutations can show similar *EoA*.

We emphasize that N_0/g can be a good predictor of mean adaptive trajectories (Fig. 6) but not necessarily of the trait-distributions (Fig. S10). In other words, populations with markedly different absolute sizes but similar N_0/g can use beneficial mutations of different effect sizes to arrive at similar mean *EoA* values in a given amount of time (Fig. S10). This explains how populations that are different in terms of absolute sizes can show similar *EoA* trajectories. Since fixation probabilities associated with individual mutations determine how trait distributions change over time during adaptation (Heffernan and Wahl, 2002; Patwa and Wahl, 2008), the above results also suggest that knowing the fixation probabilities may not enable one to predict *EoA* trajectories.

Conventional measures have overestimated the effective population size for adaptation.

Our findings have major implications for comparing results across experimental evolution studies. Adaptive dynamics in asexuals are highly influenced by the beneficial mutation supply rate in the population (U_bN_e), where U_b is the rate of spontaneous occurrence of beneficial mutations per individual per generation and N_e is the effective population size (reviewed in (Sniegowski and Gerrish, 2010)). In the context of a given environment, it can be assumed that U_b is a constant fraction (k) of μ, such that $U_b = k\mu$. As shown above, $\mu N_0/g$ is an approximate measure of the number of new variants created per generation that are expected to survive

bottlenecking (if the arrival times of mutations and competition across mutations are ignored). Therefore it is expected that the quantity $k\mu N_0/g$ would reflect the beneficial mutational supply per generation. Therefore, by definition, $k\mu(N_0/g) \approx U_b N_e$, which implies that $N_e \approx N_0/g$ (since $U_b = k\mu$). Unfortunately, N_0/g is an overestimate of N_e because $\mu N_0/g$ overestimates the number of new variants created per unit time by ignoring the arrival times of mutations and mutational competition. However, since $N_0\, g$ is g^2 times larger than N_0/g, and g typically varies between 3 and 20 in most experimental evolution studies (Kawecki *et al.*, 2012), it is clear that the traditional formula for *HM* can overestimate the adaptive effective population size by 1 to 2 orders of magnitude. Moreover, since the number of competing beneficial mutations per generation (a measure of the intensity of clonal interference) varies positively with N_e (Sniegowski and Gerrish, 2010), our study highlights that the conventional formula also overestimates the extent of clonal interference in periodically bottlenecked populations which can potentially complicate the interpretation of empirical studies on this topic (Desai *et al.*, 2007). Furthermore, our results can be used to explain some of the previously observed discrepancies in terms of adaptive effective population sizes in experimental evolution studies. For example, a recent study found that three experimental asexual populations with similar values of $N_0 g$ could show significantly different evolutionary dynamics (Raynes *et al.*, 2014). Our study suggests that the observed differences in the evolutionary outcomes might be explained by the fact that these populations differed remarkably from each other in terms of N_0/g. We also propose that *AS* $(=N_0/g)$ should be used to compare different studies in terms of the reported average speed or extent of adaptation in meta-analyses of laboratory evolution of asexual populations. We resolve the adaptively relevant size of such populations into two components (N_0 *and* g) based on their effects on *EoA*. Since our study demonstrates how the

relationship of *EoA* with N_0 is opposite to its relationship with *g*, these results should be useful in predicting how much adaptive change can be expected from different experimental designs. For example, decisions on culture volumes (well-plates versus flasks) and dilution ratios in laboratory evolution can be made on the basis of the above results to best suit the demands of the experiment.

Evolution of carrying capacity can feedback into adaptive trajectories.

Finally, we point out that both our experiments and simulations demonstrate that carrying capacity (*K*) can evolve during adaptation in asexual microbes (Fig. 1a and 2a). Most models of microbial adaptation do not take into account such adaptive changes in carrying capacity (Gerrish and Lenski, 1998; Desai *et al.*, 2007; Wahl and Gerrish, 2001; Campos and Wahl, 2010) despite there being clear empirical evidence that carrying capacity can change during adaptation (Novak *et al.*, 2006). Moreover, if the carrying capacity itself changes during the experiment, the constancy of bottleneck ratio (unchanging value of *g*) ensures that N_0 also changes concomitantly as the population evolves. This means that the periodicity of bottlenecks introduces a positive feedback during evolution if *K* increases adaptively – larger value of N_0 would make a population evolve higher *K*, which in turn would increase the next N_0, and so on. We think that this aspect of fitness should not be omitted from theoretical models of how microbes evolve, particularly under resource limited conditions, which are a common feature of experimental evolution protocols (Kawecki *et al.*, 2012; Lenski *et al.*, 1991).

Author contributions

Y.D.C. and S.D. conceived and designed the study. Y.D.C. conducted the experiments. S.D., S.I.A., and Y.D.C. developed the model. S.I.A. wrote the model-code. Y.D.C. ran the simulations. Y.D.C. and S.D. wrote the paper.

.

Acknowledgements

We thank Milind Watve, M.S. Madhusudhan, Shraddha Karve and Sachit Daniel for their invaluable suggestions and insightful discussions. We thank Amitabh Joshi for critical comments on an earlier draft of the manuscript. Y.D.C. was supported by a Senior Research Fellowship from Indian Institute of Science Education and Research, Pune. S.I.A. thanks Department of Science and Technology, Government of India for financial support through a KVPY fellowship. This project was supported by an external grant from Department of Biotechnology, Government of India and internal funding from Indian Institute of Science Education and Research, Pune.

References

Abdi H. (2010). Holm's sequential Bonferroni procedure. *Encycl Res Des* 1–8.

Abel S, Abel zur Wiesch P, Davis BM, Waldor MK. (2015). Analysis of Bottlenecks in Experimental Models of Infection. *PLoS Pathog* **11**: e1004823.

Barrick JE, Yu DS, Yoon SH, Jeong H, Oh TK, Schneider D, *et al.* (2009). Genome evolution and adaptation in a long-term experiment with Escherichia coli. *Nature* **461**: 1243–1247.

Campos PRA, Wahl LM. (2010). The Adaptation Rate of Asexuals: Deleterious Mutations, Clonal Interference and Population Bottlenecks. *Evolution* **64**: 1973–1983.

Campos PRA, Wahl LM. (2009). The Effects of Population Bottlenecks on Clonal Interference, and the Adaptation Effective Population Size. *Evolution* **63**: 950–958.

Charlesworth B. (2009). Effective population size and patterns of molecular evolution and variation. *Nat Rev Genet* **10**: 195–205.

De Visser J a. GM, Rozen DE. (2005). Limits to adaptation in asexual populations. *J Evol Biol* **18**: 779–788.

Desai MM, Fisher DS, Murray AW. (2007). The Speed of Evolution and Maintenance of Variation in Asexual Populations. *Curr Biol* **17**: 385–394.

Dey S, Joshi A. (2006). Stability via Asynchrony in Drosophila Metapopulations with Low Migration Rates. *Science* **312**: 434–436.

Ellstrand NC, Elam DR. (1993). Population genetic consequences of small population size: implications for plant conservation. *Annu Rev Ecol Syst* 217–242.

Eyre-Walker A, Keightley PD. (2007). The distribution of fitness effects of new mutations. *Nat Rev Genet* **8**: 610–618.

Gerrish PJ, Lenski RE. (1998). The fate of competing beneficial mutations in an asexual population. *Genetica* **102**–**103**: 127–144.

Heffernan JM, Wahl LM. (2002). The effects of genetic drift in experimental evolution. *Theor Popul Biol* **62**: 349–356.

Jiménez-Mena B, Tataru P, Brøndum RF, Sahana G, Guldbrandtsen B, Bataillon T. (2016). One size fits all? Direct evidence for the heterogeneity of genetic drift throughout the genome. *Biol Lett* **12**: 20160426.

Karve SM, Daniel S, Chavhan YD, Anand A, Kharola SS, Dey S. (2015). Escherichia coli populations in unpredictably fluctuating environments evolve to face novel stresses through enhanced efflux activity. *J Evol Biol* **28**: 1131–1143.

Kassen R, Bataillon T. (2006). Distribution of fitness effects among beneficial mutations before selection in experimental populations of bacteria. *Nat Genet* **38**: 484–488.

Katju V, Packard LB, Bu L, Keightley PD, Bergthorsson U. (2015). Fitness decline in spontaneous mutation accumulation lines of Caenorhabditis elegans with varying effective population sizes. *Evol Int J Org Evol* **69**: 104–116.

Kawecki TJ, Lenski RE, Ebert D, Hollis B, Olivieri I, Whitlock MC. (2012). Experimental evolution. *Trends Ecol Evol* **27**: 547–560.

Ketola T, Mikonranta L, Zhang J, Saarinen K, Örmälä A-M, Friman V-P, *et al*. (2013). Fluctuating Temperature Leads to Evolution of Thermal Generalism and Preadaptation to Novel Environments. *Evolution* **67**: 2936–2944.

LaBar T, Adami C. (2016). Different Evolutionary Paths to Complexity for Small and Large Populations of Digital Organisms. *bioRxiv* 49767.

Lachapelle J, Reid J, Colegrave N. (2015). Repeatability of adaptation in experimental populations of different sizes. *Proc R Soc Lond B Biol Sci* **282**: 20143033.

Lanfear R, Kokko H, Eyre-Walker A. (2014). Population size and the rate of evolution. *Trends Ecol Evol* **29**: 33–41.

Lenski RE, Rose MR, Simpson SC, Tadler SC. (1991). Long-Term Experimental Evolution in Escherichia coli. I. Adaptation and Divergence During 2,000 Generations. *Am Nat* **138**: 1315–1341.

Novak M, Pfeiffer T, Lenski RE, Sauer U, Bonhoeffer S. (2006). Experimental Tests for an Evolutionary Trade-Off between Growth Rate and Yield in E. coli. *Am Nat* **168**: 242–251.

Park S-C, Krug J. (2007). Clonal interference in large populations. *Proc Natl Acad Sci* **104**: 18135–18140.

Patwa Z, Wahl L. (2008). The fixation probability of beneficial mutations. *J R Soc Interface* **5**: 1279–1289.

Petit N, Barbadilla A. (2009). Selection efficiency and effective population size in Drosophila species. *J Evol Biol* **22**: 515–526.

Raynes Y, Gazzara MR, Sniegowski PD. (2012). Contrasting Dynamics of a Mutator Allele in Asexual Populations of Differing Size. *Evolution* **66**: 2329–2334.

Raynes Y, Halstead AL, Sniegowski PD. (2014). The effect of population bottlenecks on mutation rate evolution in asexual populations. *J Evol Biol* **27**: 161–169.

Rozen DE, Habets MGJL, Handel A, de Visser JAGM. (2008). Heterogeneous Adaptive Trajectories of Small Populations on Complex Fitness Landscapes. *PLoS ONE* **3**: e1715.

Samani P, Bell G. (2010). Adaptation of experimental yeast populations to stressful conditions in relation to population size. *J Evol Biol* **23**: 791–796.

Sniegowski PD, Gerrish PJ. (2010). Beneficial mutations and the dynamics of adaptation in asexual populations. *Philos Trans R Soc B Biol Sci* **365**: 1255–1263.

Szendro IG, Franke J, Visser JAGM de, Krug J. (2013). Predictability of evolution depends nonmonotonically on population size. *Proc Natl Acad Sci* **110**: 571–576.

533 Vogwill T, Phillips RL, Gifford DR, MacLean RC. (2016). Divergent evolution peaks under intermediate
534 population bottlenecks during bacterial experimental evolution. *Proc R Soc B* **283**: 20160749.

535 Wahl LM, Gerrish PJ. (2001). The Probability That Beneficial Mutations Are Lost in Populations with
536 Periodic Bottlenecks. *Evolution* **55**: 2606–2610.

537 Wahl LM, Gerrish PJ, Saika-Voivod I. (2002). Evaluating the impact of population bottlenecks in
538 experimental evolution. *Genetics* **162**: 961–971.

539 Wilke CO. (2004). The Speed of Adaptation in Large Asexual Populations. *Genetics* **167**: 2045–2053.

540

541

Supplementary information

Supplementary methods

Culture environment for experimental evolution:

24 independent bacterial populations *Escherichia coli* K-12 MG1655 were grown in nutrient broth with a fixed concentration of an antibiotic cocktail containing a mixture of three antibiotics at sub-lethal concentrations:

1. Norfloxacin (0.015 mg/ml)
2. Rifampicin (0.1 μg/ml)
3. Streptomycin (6 μg/ml)

The following table summarizes the numerical properties of the three population regimes used in our study:

Regime type	Starter population size	Final population size	Dilution during bottleneck	No. of generations per dilution	Harmonic mean size	Culture volume
SS	1.5x	15000x	1: 10^4	≈13.28	**~20x**	**1.5ml**
SL	x	10^6x	1:10^6	≈19.93	**~20x**	**100ml**
LL	10^5x	10^6x	1:10	≈3.32	**~3.32*10^5x**	**100ml**

Table S1. A summary of the experimental populations. x ≈ 10^5 in our experiments.

Our study design had eight biological replicates belonging to each one of the three population regimens (24 independently evolving populations). Each population was assayed in triplicates for measuring fitness using growth curves. This corresponded to 72 growth curves at a given point during the selection timeline. We performed a mixed-model ANOVA at distinct time-points (shown in Fig. 1 of Main-text) with population regimen as the fixed factor and replicate index within a regimen as the random factor nested in the fixed factor. Since we didn't wish to compare data points corresponding to the same population at different times, we did not use repeated measures ANOVA in our study. The statistical analysis was corrected for multiple tests using Holm-Šidàk correction (Abdi, 2010).

Algorithm for the individual based model used in this study:

Our model simulates the growth of individual bacteria in density-dependent resource-limited conditions. Each bacterium is represented by an array which has the following components:

1. Determinant of efficiency (K_eff): determines how much food can be assimilated per unit time

2. Determinant for threshold (thres): how much food needs to be assimilated in order to divide
3. Bodymass: how big is the bacterium (where is it along its cell cycle) at any given time

At the beginning of the simulation, two global scaling quantities, Food_Proxy and Body_Proxy are declared for the whole population. As the names suggest, Food_Proxy acts as a proxy for the amount of available resources initially, while Body_Proxy (=250) is a proxy for bodymass of the ancestor. Each simulation run is started with 100 individuals and each individual is allotted K_eff_i value given as Eff_i * Food_Proxy. Here, Eff_i is a random number picked from a uniform distribution U(0.95-1.05) and K_eff_i determines how much food would be consumed in a density–dependent manner and when its food consumption would stop (as per the conditions given below). Similarly, the parameter for threshold is assigned as a random number picked from a uniform distribution between 0.95*(Body_Proxy) and 1.05*(Body_Proxy).

Each bacterium has the same initial biomass (an arbitrarily small quantity, 10 units in this case).

Time is implicitly defined in our code and each iteration signifies one unit of time.

In each iteration, each bacterium "grows and divides" according to the following rules:

If for bacterium i, (population size/ K_eff_i) ≥ 1, it doesn't eat anything: its bodymass remains the same as the earlier iteration.

If for bacterium i (population size/ K_eff_i) < 1, it eats 10(1 - (population size/ K_eff_i)) units of food in this iteration: its bodymass increases by 1- (population size/ K_eff_i) units.*

If at the end of this iteration, $bodymass_i > thres_i$, bacterium i divides into two equal parts. A small thermodynamic cost (constant for all individuals) is deducted so that the sum of the bodymass of the daughter cells is exactly 1 unit less than the bodymass of the mother cell at the time of division.

If the bacterium divides, there is a 1 in 100 chance for each of the daughter cells that it mutates. If a mutation occurs, the new parameter for efficiency is drawn from an already defined normal distribution that is used throughout the simulation. The same applies to threshold. (Threshold and efficiency mutate independently in each bacterium.)

The total size of the population is saved at the end of every iteration. The total amount of food consumed during each iteration is also computed.

The above description (italics) represents all the processes that happen within an iteration.

The process is repeated (and the population grows) until the following conditions are fulfilled:

1. The number of iterations is greater than 2000.
2. The amount of food consumed during each iteration < 0.08* Food_Proxy

If the above conditions are met simultaneously, food consumption is stopped, a defined fraction of individuals are sampled randomly and the whole process is started with this sample population (this represents bottlenecking). The above process is continued for *q* bottlenecks. The bottleneck ratio and the number *q* are predefined, depending upon the type of population being studied. This gives rise to *q* sigmoidal growth curves. Two quantities are extracted from each sigmoidal curve:

1. Carrying capacity (*K*, the maximum size of the population in each growth phase)
2. Maximum linear growth rate (*R*, the maximum slope of population growth over 100 iterations). Straight lines were fit on overlapping moving windows of 100 iterations on the entire time-series of population size values within each growth-phase. The maximum value of the slope observed within the entire time-series of population size values (sigmoidal curve) was taken to be the maximum growth rate (*R*).

Time series of carrying capacities and maximum growth rates are computed using the series of q sigmoidal curves.

In each simulation used in this study, the carrying capacity of the first growth phase was ≈ 1.8*Food_Proxy. The value of Food_Proxy was adjusted in such a way that it gave rise to the desired value of the carrying capacity of the first growth phase in a simulation. The carrying capacities corresponding to the subsequent growth phases was an emergent result of Darwinian evolution in the simulations.

The following simulation settings were used in our study:

Population type	Food_proxy	Bottleneck ratio	Number of bottlenecks (400 generations)
XX'	$2*10^4$	1/10	120
SS'	10^5	$1/10^2$	60
SL'	$5*10^6$	$1/10^4$	30
BN1	$5*10^3$	1/10	120
BN2	$5*10^4$	$1/10^2$	60
BN3	$5*10^5$	$1/10^3$	40
BN4	$5*10^6$	$1/10^4$	30
SM1	$5*10^3$	1/10	120
SM4	$5*10^6$	$1/10^4$	30
HB	$5*10^6$	$1/10^4$	30
LB	$2*10^4$	1/10	120
LBbar	$1.25*10^3$	1/10	120
MBbar	$2.5*10^4$	1/100	60

We checked if our simulations met several other theoretical expectations from the extant literature. As expected, despite following the same distribution for mutations, large populations showed curves of diminishing returns while adapting whereas very small populations showed stepwise increase in fitness with long periods of stasis (Fig. S2). This happens because very small populations (but not large ones) need to wait for beneficial mutations to arise (Sniegowski and Gerrish, 2010). Moreover, the extent of adaptation showed a positive but saturating relationship with an unambiguous measure of absolute population size in our simulations (Fig. S6a and S6b). The simulations also revealed a non-monotonous relationship between fitness and mutation rate (Orr, 2000) (Fig. S7).

637 **Table S2. Distributions for parameters used in simulations:**

638

Distribution used for	Distribution for efficiency parameter	Distribution for threshold parameter
Starting the simulation	Uniform random(0.95,1.05)	Uniform random(237.5,262.5)
Mutation	Normal random (0.9,0.22)	Normal random (1.1,0.22)

639

640

641

642 **Supplementary Data:**

643 **Statistical analysis of empirical results**

644

Generation	ANOVA F	ANOVA p	Holm-Šidàk corrected *p*	Tukey p LL-SL	Tukey p LL-SS	Tukey p SL-SS
40	36.75	1.4E-7	1E-6	0.0001	0.0001	0.0001
80	13.319	0.0002	0.0011	0.0001	0.0001	0.7942
120	14.365	0.0001	0.0008	0.0001	0.0001	0.0001
160	17.282	3.7E-5	0.0003	0.0001	0.0001	0.0001
200	2.894	0.0776	0.0776	-	-	-
240	9.359	0.0012	0.0050	0.0001	0.0001	0.0001
280	12.110	0.0003	0.0016	0.0001	0.0001	0.0001
320	6.769	0.0054	0.0161	0.0001	0.0001	0.0001
~ 390	3.33	0.0556	0.1081	-	-	-

645

646 **Table S3. A summary of statistical analysis of carrying capacity measurements in empirical**
647 **populations.** The values in red represent statistically significant difference ($p<0.05$). The *p*-
648 values corresponding to nine independent ANOVAs (corresponding to nine different time points)
649 were subjected to Holm-Šidàk correction. Post-hoc (Tukey) comparisons were done only in
650 cases where the ANOVA *p*-values were less than 0.05 after Holm-Šidàk correction. These post –
651 hoc comparisons were done across the three experimental regimens (LL, SL, and SS) at each
652 time point. Holm-Šidàk correction was not done on Tukey *p*-values. The *p*-values are reported to
653 four decimal places.

Generation	ANOVA F	ANOVA p	Holm-Šidàk corrected p	Tukey p LL-SL	Tukey p LL-SS	Tukey p SL-SS
40	56.631	3.5E-9	3.1E-8	0.0001	0.0001	0.0001
80	5.996	0.0087	0.0344	0.0001	0.0001	0.3229
120	12.027	0.0003	0.0023	0.0001	0.0001	0.0001
160	12.287	0.0003	0.0023	0.0001	0.0001	0.0001
200	3.093	0.0665	0.1286	-	-	-
240	8.757	0.0017	0.0103	0.0001	0.0001	0.0001
280	7.785	0.0030	0.0147	0.0001	0.0001	0.0001
320	4.096	0.0315	0.0915	-	-	-
~ 390	0.925	0.4122	0.4122	-	-	-

Table S4. A summary of statistical analysis of maximum growth rate measurements in empirical populations. The values in red represent statistically significant difference ($p<0.05$). The values in red represent statistically significant difference ($p<0.05$). The *p*-values corresponding to nine independent ANOVAs (corresponding to nine different time points) were subjected to Holm-Šidàk correction. Post-hoc (Tukey) comparisons were done only in cases where the ANOVA *p*-value was less than 0.05 after Holm-Šidàk correction. These post –hoc comparisons were done across the three experimental regimens (LL, SL, and SS) at each time point. Post-hoc comparisons were never performed across time-points (generations). The *p*-values are reported to four decimal places.

Agreement between experiments and simulations

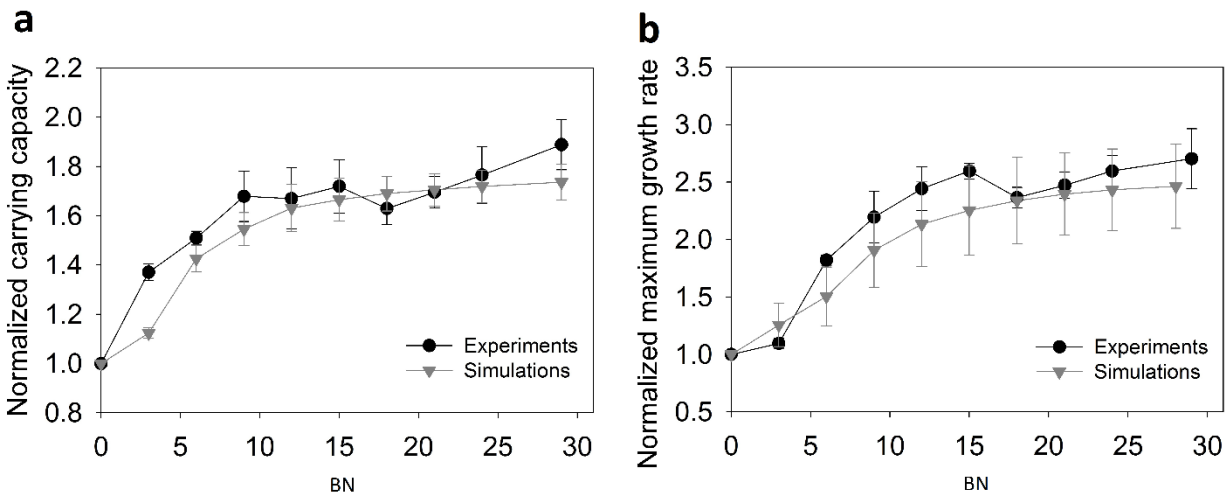

Fig. S1. Agreement between experiments and simulations in terms of adaptive dynamics over identical time-scales in numerically similar populations. (**a**) Carrying capacity *(K)* versus bottleneck number *(BN)* (**b**) Maximum growth rate *(R)* versus bottleneck number *(BN)*. Data points represent mean ± SD over 8 replicates. Each data point corresponds to the respective measure of fitness *(K or R)* derived from the sample taken after *BN* bottlenecks. Range of population size: $N_0 \approx 10^{4.5}$; $N_f \approx 10^{8.5}$; bottleneck ratio = $1/10^4$. Each bottleneck corresponds to approximately 13.28 generations. Carrying capacity is normalized with the ancestral value.

The results of our experiments and simulations agree well in terms of the range and dynamics of adaptation over identical time-scales in numerically similar populations. This applies to both measures of population-level fitness: carrying capacity *(K)* and maximum growth rate *(R)*.

Qualitative differences in EoA trajectory-shapes brought about by large differences in population size

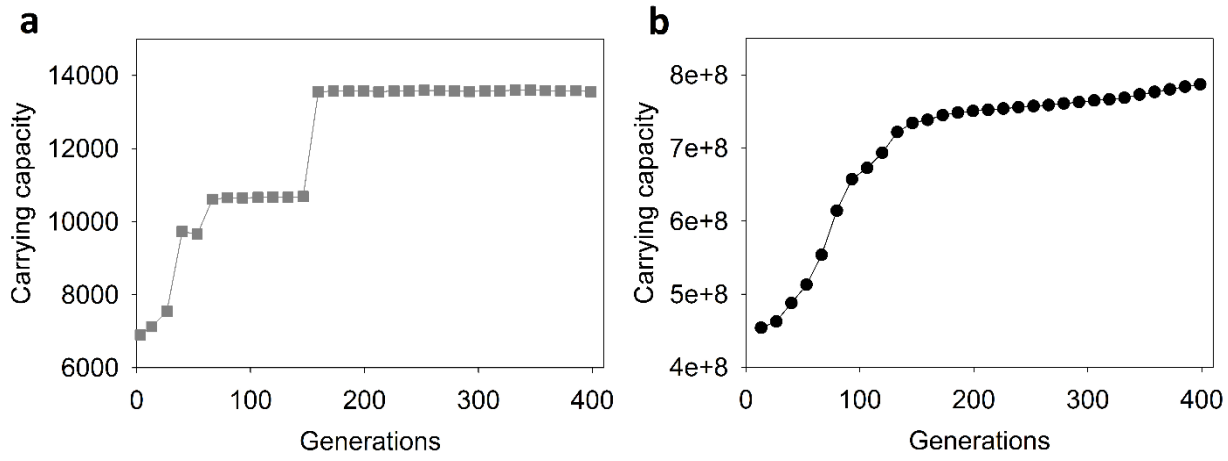

Fig. S2. Qualitative differences in adaptive trajectories corresponding to populations with a large different in their sizes. Stepwise increase in fitness (with long periods of stasis) occurred in typically small populations such as the one shown in (**a**) as compared to smooth curves of diminishing returns in typically large populations such as the one shown in (**b**) (See the ordinates for absolute ranges of N_f during adaptation). The population shown in (**a**) experienced a periodic bottleneck of 1/10 while he population shown in (**b**) was bottlenecked $1/10^4$ periodically.

As expected (Sniegowski and Gerrish, 2010), very small populations showed staicase-like (stepwise) trajectories of fitness increase.

Changes in standard deviation with sample size

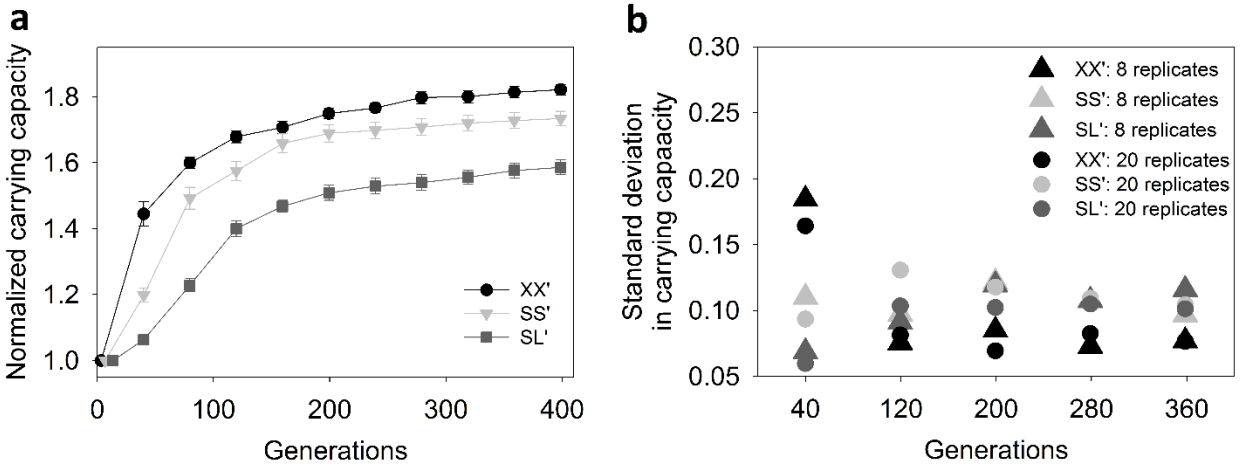

Fig. S3. Increasing the number of replicate simulations from 8 to 20 did not result in increase in variation across replicates. (**a**) Increasing the number of independent replicate simulations from 8 to 20 didn't result in qualitative changes (ranks) of three populations with similar harmonic mean size but different N_0/g (mean ± SEM; N=20) (compare with Fig. 2a in the Main-text). (**b**) This increase in replicate number also didn't result in major changes in the standard deviation in carrying capacity during the course of adaptation. XX': $N_0 \approx 3.6*10^3$, bottleneck ratio: 1/10; SS': $N_0 \approx 1.8*10^3$, bottleneck ratio: $1/10^2$; SL': $N_0 \approx 9*10^2$, bottleneck ratio: $1/10^4$.

Since our simulations are agent-based (and consequently take a very long time to run), we decided to operate on a sample size of 8 replicates per population type throughout our study.

Adaptation in terms of efficiency and threshold:

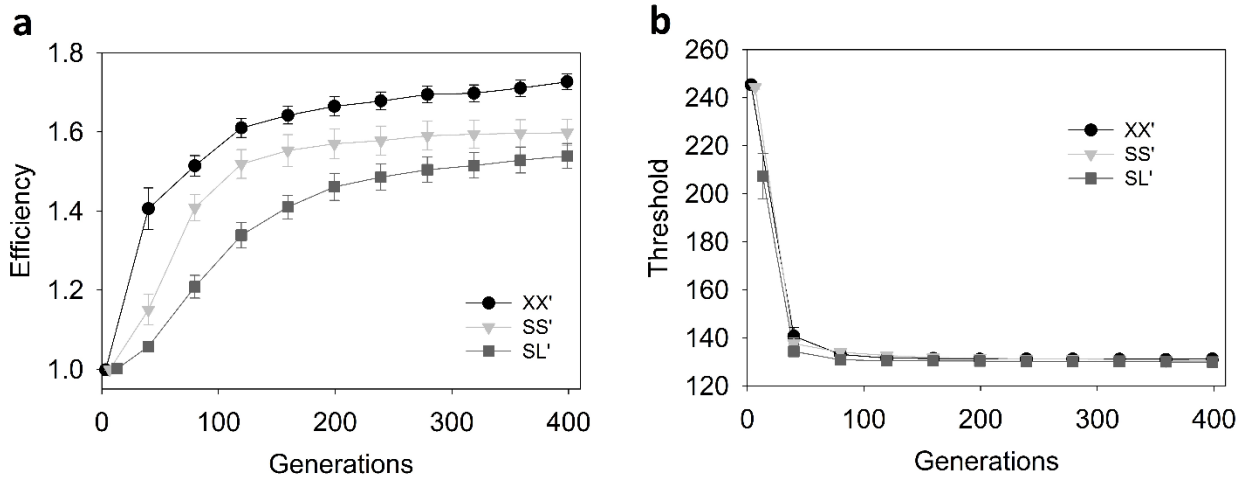

Fig. S4. Adaptation in three populations with similar HM in terms of measures of fitness at the level of individuals (**a**) Adaptive increase in averge individual efficiency within populations with similar harmonic mean size (mean ± SEM; 8 replicates). (**b**) Adaptive decrease in average individual threshold in populations with similar harmonic mean size (mean ± SEM; 8 replicates). Threshold evolved so quickly that its adaptive decrease did not refelct the differnce observed in *EoA* trjectories for *K* and *R* (Fig. 2 (Main text)). XX': $N_0 \approx 3.6*10^3$, bottleneck ratio: 1/10; SS': $N_0 \approx 1.8*10^3$, bottleneck ratio: $1/10^2$; SL': $N_0 \approx 9*10^2$, bottleneck ratio: $1/10^4$.

Multiple measures of fitness in our study revealed that harmonic mean is not a good predictor of adaptive trajectories because populations with similar harmonic mean size can have markedly different adaptive trajectories (Fig. S4 and Fig. 2 (Main-text)). Identical trends were observed when such populations (XX', SS', and SL') were compared in terms of two different measures of population level fitness (Fig. 2 (Main-text)). In terms of fitness at the level of individuals, efficiency showed the same trend as *R* and *K* (Figu. S4a). However,the adaptive trajectories corresponding to XX', SS', and SL' were almost identical when expressed in terms of threshold. Threshold evolved (decreased) so quickly and to such a large extent in almost all population types that we simulated in this study (regardless of their HM) that most populations had similar trajectories of threshold decrease (also see Fig. S6d). Consequently, despite threshold being an important determinant of fitness, adaptive differences amongst populations were best expressed and explained in terms of trajectories of increase in efficiency and not in terms of decrease in threshold. The trends shown by adaptive trajectories of efficiency increase were identical to those shown by adaptive trajectories of *K* and *R*. Due to the above reasons, we focussed on population-wide trait distributions only in terms of efficiency.

741 **Adaptive changes in distributions of efficiency in populations with similar HM:**

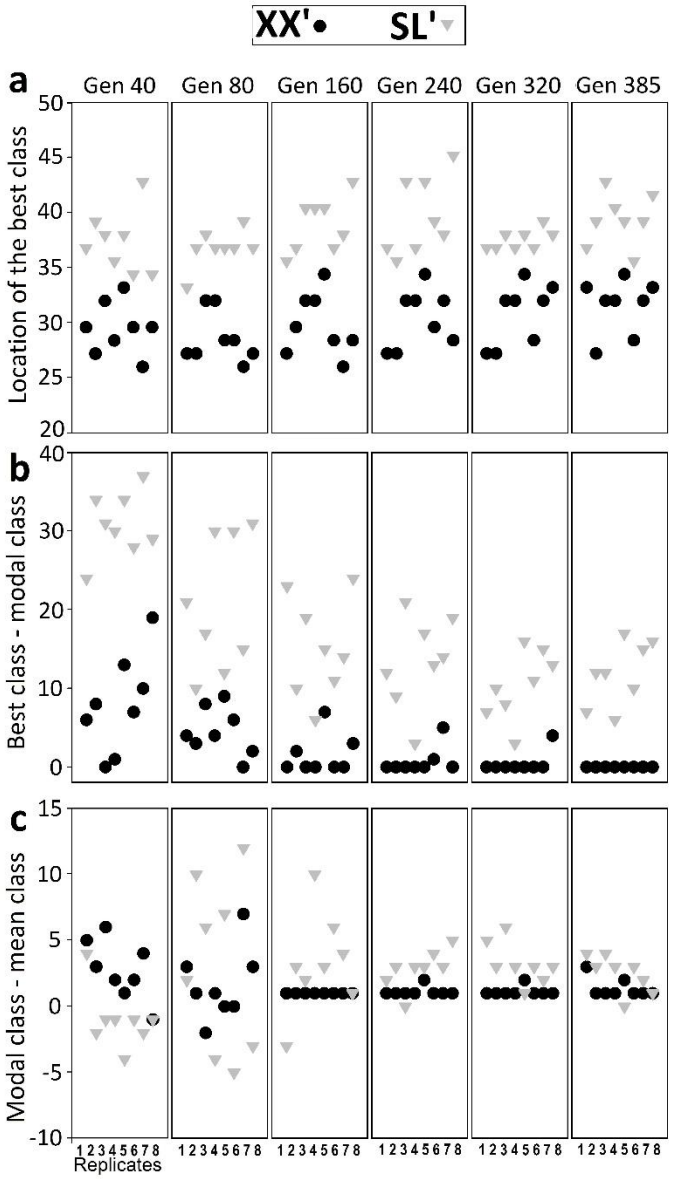

742

743 **Fig. S5. The distributions of efficiency across constituent individuals during adaptation in**
744 **populations with similar HM.** The individuals of each simulated population (8 replicate
745 populations each of XX' and SL') were classified into to a discrete frequency distribution of
746 their efficiency values (50 static classes). Higher class indices correspond to higher efficiencies.
747 The best phenotype (in terms of fitness) explored by SL' was consistently fitter than the best
748 phenotype explored by LB (**a**). The modal phenotype quickly converged with the best available
749 phenotype in most XX' populations but failed to do so in all SL' populations (**b**). The mean
750 phenotype in XX' approached the best phenotype very closely (**b** and **c**). However, there was a
751 consistently larger gap between the best phenotype and the modal phenotype in SL' (**b**) and an
752 even larger one between its best and mean phenotype (**b** and **c**).

Our simulations revealed that populations with similar harmonic mean size can differ appreciably from each other not only in terms of their adaptive trajectories but also in terms of how the distribution of fitness amongst their constituent individuals changes during adaptation.

Relationship of *EoA* with N_0 and *g*

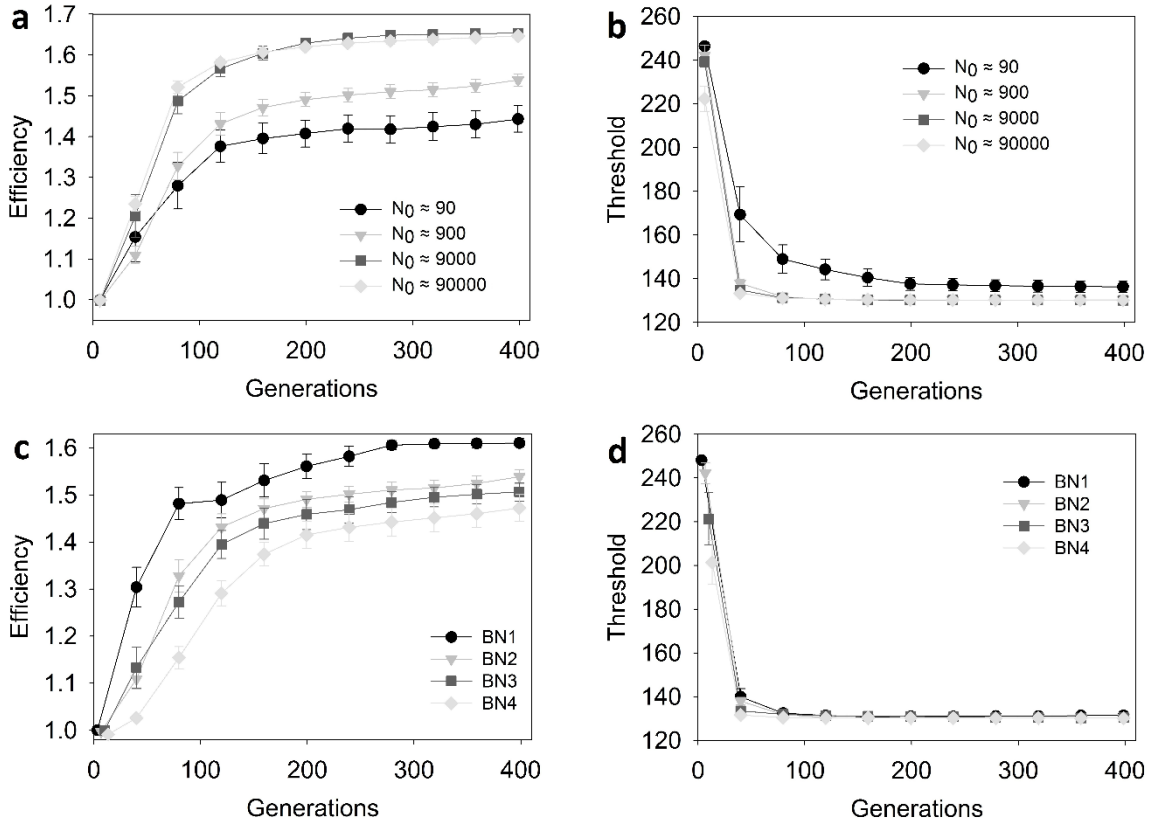

Fig. S6. The relationship of *EoA* with N_0 and *g*. *EoA* exhibited a positive and saturating relationship with N_0 (**a** and **b**) but a negative relationship with g (**c**). The data points show mean ± SEM (N=8). The populations shown in **a** and **b** were bottlenecked $1/10^2$ periodically. The populations shown in C and D had $N_0 \approx 900$. Bottleneck ratios: BN1: 1/10; BN2: $1/10^2$; BN3: $1/10^3$; BN4:$1/10^4$.

As predicted by the extant theory (Wahl and Gerrish, 2001; Campos and Wahl, 2009), the extent of adaptation (*EoA*) had a positive but saturating relationship with N_0. However, we found that *EoA* varied negatively with *g*. Populations with similar N_0 but different g had markedly different adaptive trajectories (Fig. S6C and Fig. 3, 4 (Main-text)).

769 **Relationship between *EoA* and *g* at three different mutation rates:**

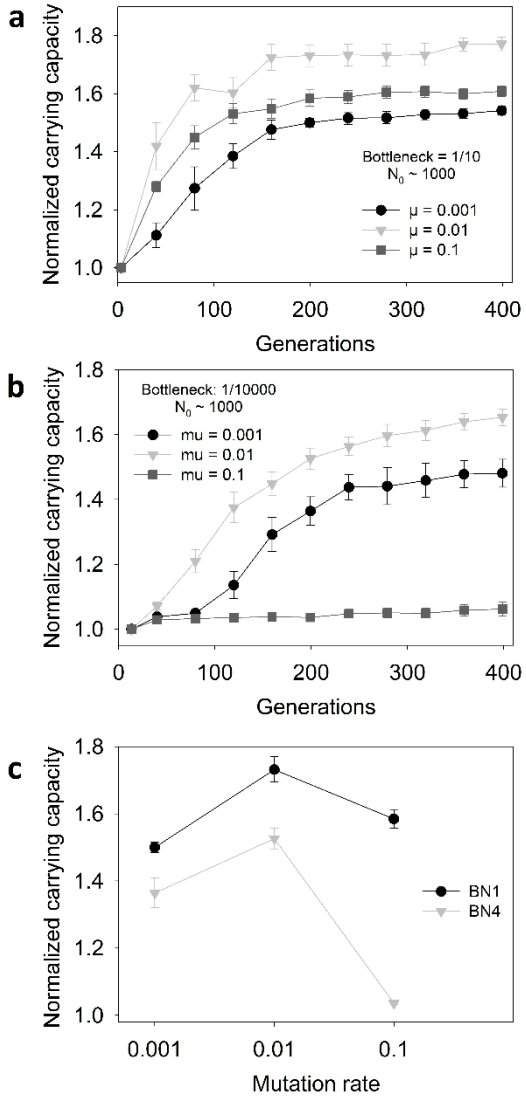

770

771 **Fig. S7. The negative relationship between *EoA* and *g* was robust to changes in mutation**
772 **rate.** (**a**) Adaptive increase in normalized carrying capacity in BN1 populations at three mutation
773 rates. (**b**) Adaptive increase in normalized carrying capacity in BN4 populations at three
774 mutation rates. (**c**) Normalized carrying capacity in BN1 and BN4 at generation 200 at three μ
775 values. *EoA* exhibited a non-monotonous relationship with μ in both BN1 and BN4 populations,
776 which is in line with theoretical expectations (Orr, 2000). The negative dependence of *EoA* on *g*
777 was robust to changes in mutation rate *(μ)* over a 100-fold range. We found that the relationship
778 between *EoA* and μ can be influenced by bottleneck ratio. This is in agreement with recent
779 empirical findings (Raynes *et al.*, 2014). The data points show mean ± SEM (8 replicates). Both
780 BN1 and BN4 had similar bottleneck size ($N_0 \approx 900$). BN1 experienced a periodic bottleneck of
781 1/10 whereas BN4 experienced a periodic bottleneck of $1/10^4$.

782

783

784 **Differences in the locations of the best class before and after bottleneck:**

785

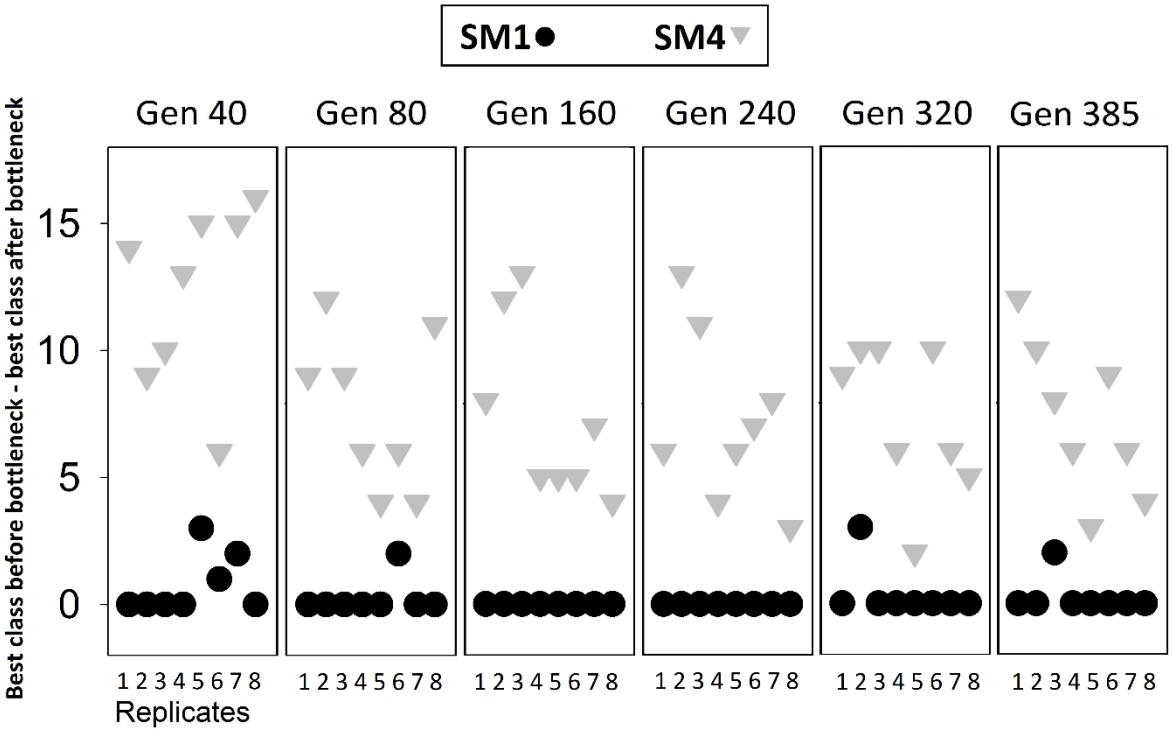

786

787 **Fig. S8. Differences in the locations of the best class in the distribution of the efficeincy**
788 **parameter before and after bottlenck.** The individuals of each simulated population (8
789 replicate populations each of SM1 and SM4) were classified into to a discrete frequency
790 distribution of their efficiency values (50 static classes). While the best class of SM1 could
791 survive the bottleneck in most cases (black circles), the best class of SM4 invariably failed to
792 survive its harsh bottleneck (grey triangles).

793

794

795

N_0/g is a better predictor of *EoA* trajectories than N_0g:

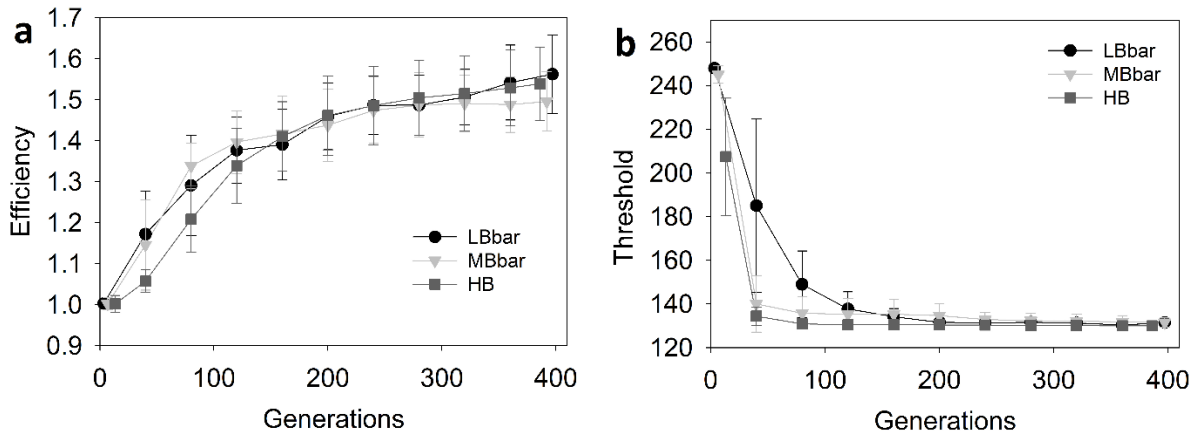

Fig. S9. Adaptive trajectories in population with similar N_0/g expressed in terms of efficiency (**a**) and threshold (**b**). The data points show mean ± SD (8 replicates). LBbar: $N_0 \approx 225$; bottleneck ratio = 1/10; MBbar: $N_0 \approx 450$; bottleneck ratio = $1/10^2$; $N_0 \approx 900$; bottleneck ratio = $1/10^4$.

Populations with similar N_0/g had remarkably similar adaptive trajectories in terms of both efficiency and threshold (Fig. S9). These populations had similar adaptive trajectories despite differing in terms of the intensity of the periodic botleneck over a 1000-fold range. While N_0*g failed to predict adaptive trajectories over this bottleneck range (Fig. 2 and 6 (Main text)), N_0/g could act as a much better predictor of adaptive trajectories.

Population with similar mean *EoA* trajectories can differ remarkably in terms of distributions of the corresponding fitness-affecting trait:

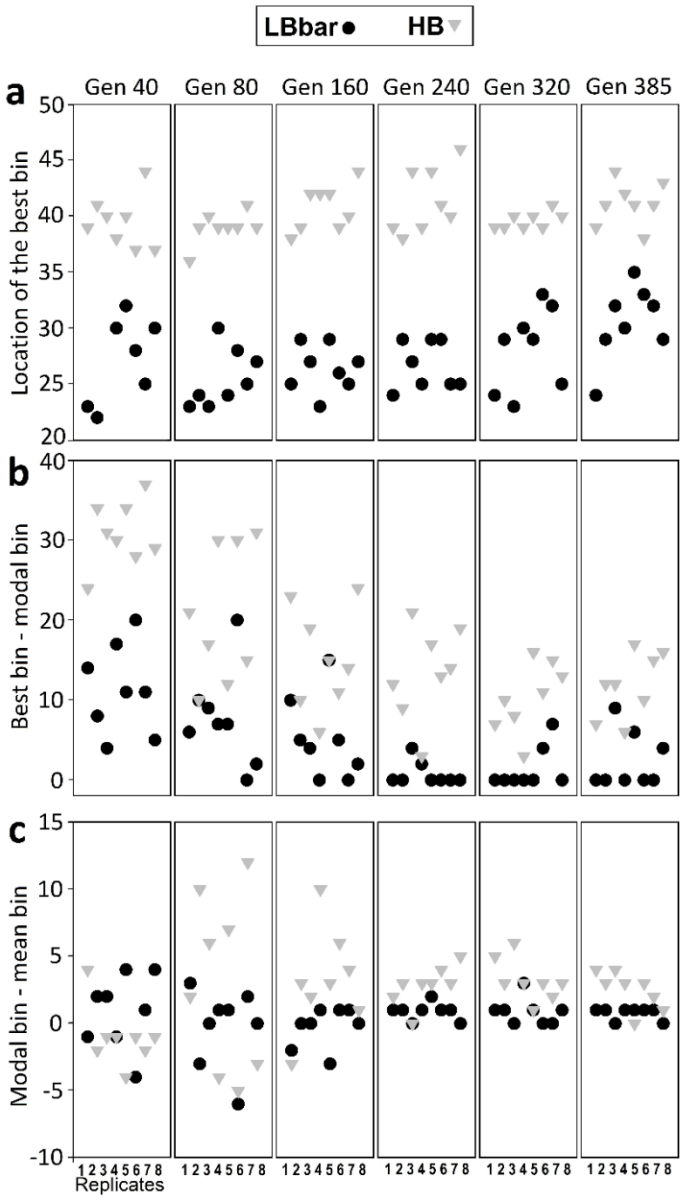

Fig. S10. The distributions of phenotypic effects across constituent individuals during adaptation in populations with similar N_0/g. The individuals of each simulated population (8 replicate populations each of LBbar and HB) were classified into to a discrete frequency distribution of their efficiency values (50 static bins). Higher bin indices correspond to higher efficiencies. The best phenotype (in terms of fitness) explored by HB was consistently fitter than the best phenotype explored by LBbar (**a**). The modal phenotype quickly converged with the best available phenotype in most LBbar populations but failed to do so in all HB populations (**b**). The mean phenotype in LBbar approached the best phenotype very closely (**b** and **c**). However, there was a consistently larger gap between the best phenotype and the modal phenotype in HB (**b**) and an even larger one between its best and mean phenotype (**b** and **c**).

Poulations that have similar mean adaptive trajectories can nevertheless have remarkably different distribution of fitness amongst their constituent individuals, and can also differ in terms of how these distributions themselves change over time. LBbar and HB have markedly different distributions of fitness amongst their constituent individuals during the course of adaptation, despite having similar fitness trajectories.

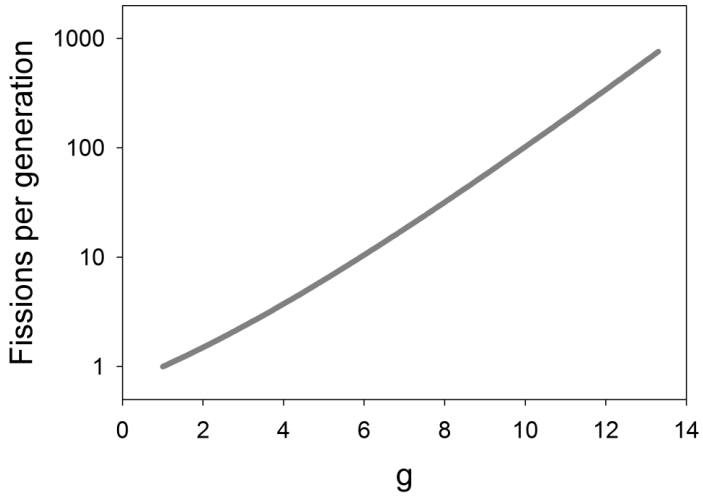

Fig. S11. The frequency of binary fissions per generation as a function of *g*. $N_0*(2^g-1)/g$ represents the number of binary fissions per generation.

References to Supplementary Information

1. Abdi H. Holm's sequential Bonferroni procedure. Encycl Res Des. 2010;1–8.

2. Sniegowski PD, Gerrish PJ. Beneficial mutations and the dynamics of adaptation in asexual populations. Philos Trans R Soc B Biol Sci. 2010 Apr 27;365(1544):1255–63.

3. Orr HA. The Rate of Adaptation in Asexuals. Genetics. 2000 Jun 1;155(2):961–8.

4. Wahl LM, Gerrish PJ. The Probability That Beneficial Mutations Are Lost in Populations with Periodic Bottlenecks. Evolution. 2001 Dec 1;55(12):2606–10.

5. Campos PRA, Wahl LM. The Effects of Population Bottlenecks on Clonal Interference, and the Adaptation Effective Population Size. Evolution. 2009 Apr 1;63(4):950–8.

6. Raynes Y, Halstead AL, Sniegowski PD. The effect of population bottlenecks on mutation rate evolution in asexual populations. J Evol Biol. 2014 Jan 1;27(1):161–9.